Electronic Supporting Information

Luminescent cadmium(II) coordination polymers of 1,2,4,5-tetrakis(4-pyridylvinyl)benzene used as efficient multi-responsive sensors for toxic metal ions in water

Wei-Jie Gong,[a] Rui Yao,[a] Hong-Xi Li,*[a] Zhi-Gang Ren,[a] Jian-Guo Zhang[a] and Jian-Ping Lang*[ab]

[a] College of Chemistry, Chemical Engineering and Materials Science, Soochow University, Suzhou 215123, People's Republic of China

[b] State Key Laboratory of Organometallic Chemistry, Shanghai Institute of Organic Chemistry, Chinese Academy of Sciences, Shanghai 200032, People's Republic of China

Table of Contents

Table S1 Selected bond lengths (Å) and angles (°) for **1, 2** and **3**.....S3

Fig. S1 PXRD patterns for **1** (a), **2** (b) and **3** (c). Simulated (black) and single-phase polycrystalline sample (red).....S4

Fig. S2 (a) View of the coordination environment of the Cd(II) center in **2** with 45% thermal ellipsoids and all hydrogen atoms are omitted for clarity. Symmetry codes: (A) *x*, *y* - 1, *z* + 1; (B) – *x* + 1, - *y*, - *z* + 1; and (C) - *x*+ 2, - *y*, - *z* + 1. (b) View of a section of the 1D double chain $[Cd_2(1,3,5\text{-HBTC})_2]_n$ extending along the *a* axis. (c) View of a 2D network of **2** extending along the [0,1,1] plane. S5

Fig. S3 View of 3D structure assembled by the π-π stacking interactions in **1** S6

Fig. S4 View of O–H···N hydrogen bonds between two layers of **2**.....S6

Fig. S5 Alignment of the neighboring 4-tkpvb ligands in **1** S7

Fig. S6 Alignments of the neighboring 4-tkpvb ligands in **2**.....S7

Fig. S7 View of 3D structure assembled by the π-π stacking interactions in **3** S7

Fig. S8 Linear region of fluorescence intensity for the 4-tkpvb solution and the suspensions of **1** in water upon incremental addition of Hg^{2+}, CrO_4^{2-} or $Cr_2O_7^{2-}$ solutions: (a) 4-tkpvb-Hg^{2+}; (b) **1**-Hg^{2+}; (c) **1**-CrO_4^{2-}; (d) **1**-$Cr_2O_7^{2-}$.....S8

Table S2 Calculation of Detection Limit (LOD).....S8

Fig. S9 PXRD patterns of MPs of **1**.....S9

Fig. S10 Emission spectra of **1** dispersed in water upon addition of inorganic metal ions (a) and anions (b) S9

Fig. S11 Concentration-dependent luminescence quenching of **1** after adding different concentrations of CrO_4^{2-} (a) and $Cr_2O_7^{2-}$ (b).....S10

Fig. S12 PXRD patterns for **1** after the detection of Hg^{2+}, CrO_4^{2-} and $Cr_2O_7^{2-}$in water S10

Fig. S13 Emission spectra of **1** with different concentrations of $Cr_2O_7^{2-}$ covering the excitation light (a) and the emission light (b) S11

Table S1 Selected bond lengths (Å) and angles (°) for **1**, **2** and **3**.

Compound **1**					
Cd(1)-N(1)	2.304(4)	Cd(1)-O(2C)	2.315(5)	Cd(1)-N(3A)	2.320(4)
Cd(1)-O(1)	2.322(4)	Cd(1)-O(3B)	2.365(4)	Cd(1)-O(4B)	2.427(4)
N(1)-Cd(1)-O(2C)	90.35(15)	N(1)-Cd(1)-N(3A)	167.15(14)	O(2C)-Cd(1)-N(3A)	95.33(15)
N(1)-Cd(1)-O(1)	85.26(13)	O(2B)-Cd(1)-O(1)	129.68(19)	N(3A)-Cd(1)-O(1)	82.23(14)
N(1)-Cd(1)-O(3B)	95.27(15)	O(2C)-Cd(1)-O(3B)	78.1(2)	N(3A)-Cd(1)-O(3B)	97.18(15)
O(1)-Cd(1)-O(3B)	152.24(15)	N(1)-Cd(1)-O(4B)	97.34(14)	O(2C)-Cd(1)-O(4B)	132.48(19)
N(3A)-Cd(1)-O(4B)	87.32(14)	O(1)-Cd(1)-O(4B)	97.74(15)	O(3B)-Cd(1)-O(4B)	54.59(15)
Compound **2**·0.5DMF					
Cd(1)-O(2B)	2.246(4)	Cd(1)-N(1)	2.302(5)	Cd(1)-O(1)	2.308(4)
Cd(1)-N(3A)	2.307(5)	Cd(1)-O(6C)	2.310(5)	Cd(1)-O(5C)	2.491(5)
O(2B)-Cd(1)-N(1)	88.14(17)	O(2B)-Cd(1)-O(1)	130.72(18)	N(1)-Cd(1)-O(1)	90.69(17)
O(2B)-Cd(1)-N(3A)	87.28(17)	N(1)-Cd(1)-N(3A)	173.2(2)	O(1)-Cd(1)-N(3A)	88.53(17)
O(2B)-Cd(1)-O(6C)	141.87(16)	N(1)-Cd(1)-O(6C)	91.66(19)	O(1)-Cd(1)-O(6C)	87.41(17)
N(3A)-Cd(1)-O(6C)	95.02(18)	O(2B)-Cd(1)-O(5C)	87.56(16)	N(1)-Cd(1)-O(5C)	90.98(18)
O(1)-Cd(1)-O(5C)	141.72(17)	N(3A)-Cd(1)-O(5C)	93.79(18)	O(6C)-Cd(1)-O(5C)	54.31(15)
Compound **3**					
Cd(1)-N(1)	2.328(4)	Cd(1)-N(1A)	2.328(4)	Cd(1)-O(1)	2.348(4)
Cd(1)-O(1A)	2.348(4)	Cd(1)-O(2)	2.399(3)	Cd(1)-O(2A)	2.399(3)
N(1)-Cd(1)-N(1A)	180(19)	N(1)-Cd(1)-O(1)	89.26(15)	N(1A)-Cd(1)-O(1)	90.74(15)
N(1)-Cd(1)-O(1A)	90.74(15)	N(1A)-Cd(1)-O(1A)	89.26(15)	O(1)-Cd(1)-O(1A)	180(2)
N(1)-Cd(1)-O(2)	88.99(13)	N(1)-Cd(1)-O(2A)	91.01(13)	O(1)-Cd(1)-O(2)	55.27(15)
O(1A)-Cd(1)-O(2)	124.73(15)	N(1A)-Cd(1)-O(2)	91.01(13)	N(1A)-Cd(1)-O(2A)	88.99(13)
O(1)-Cd(1)-O(2A)	124.73(15)	O(1A)-Cd(1)-O(2A)	55.27(15)	O(2)-Cd(1)-O(2A)	180(2)

Symmetry codes: (A) x, $y + 1$, $z - 1$; (B) $x - 1$, y, z; and (C) $-x + 1$, $-y + 1$, $-z$. for **1**. (A) x, $y - 1$, $z + 1$; $-x + 1$, $-y$, $-z + 1$; and (C) $-x + 2$, $-y$, $-z + 1$. for **2**. (A) $-x + 1$, $-y$, $-z$. for **3**.

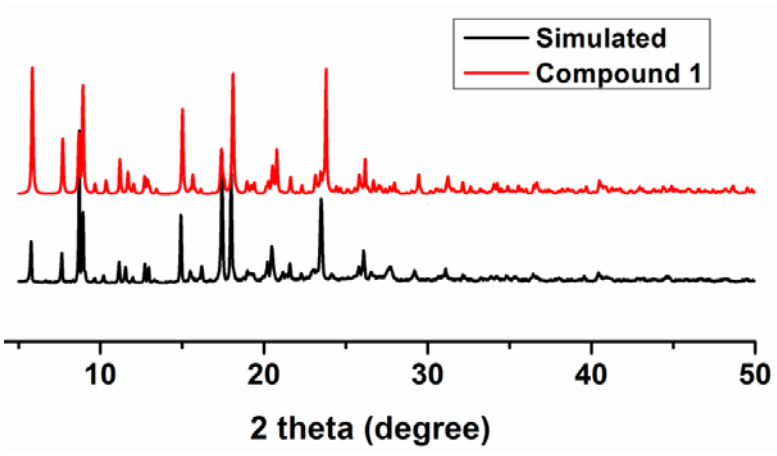

(a)

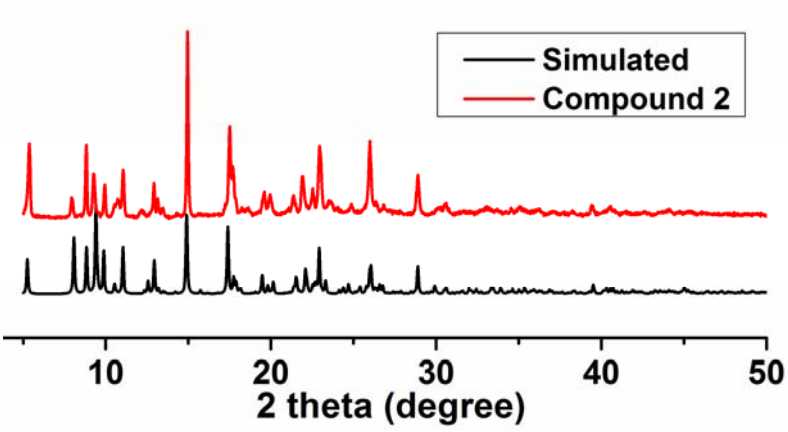

(b)

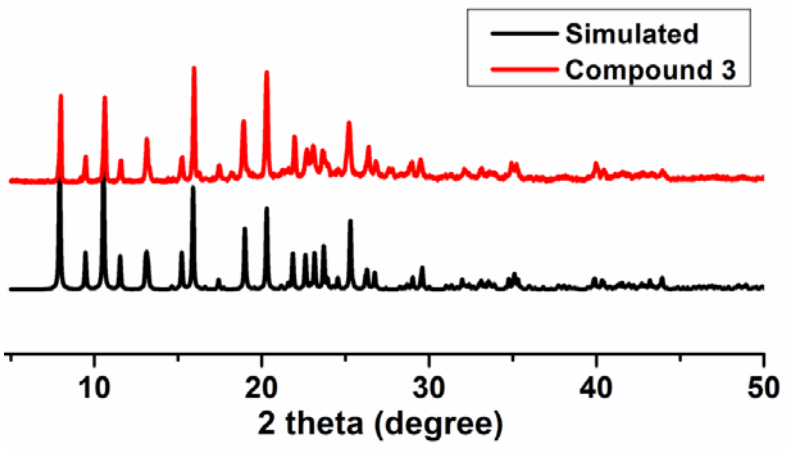

(c)

Fig. S1 PXRD patterns for **1** (a), **2** (b), and **3** (c). Simulated (black) and single-phase polycrystalline sample (red).

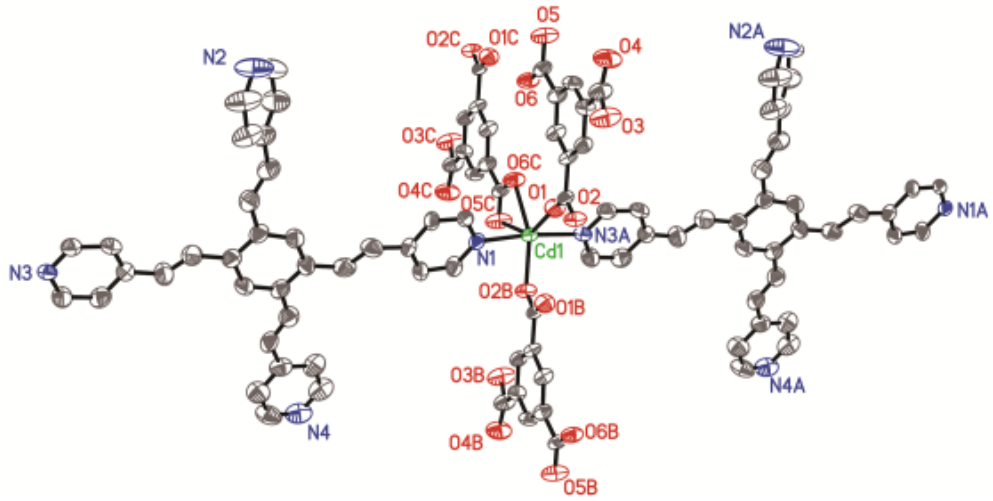

(a)

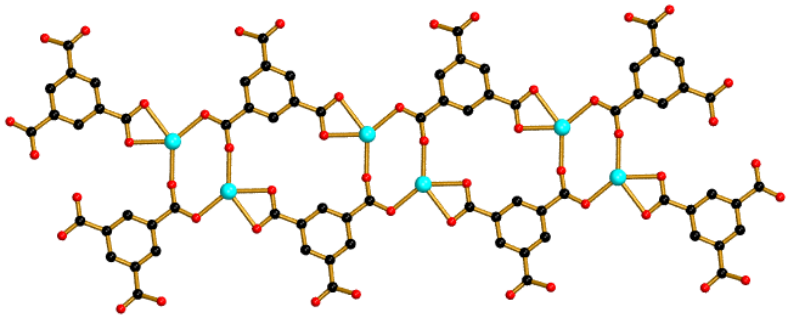

(b)

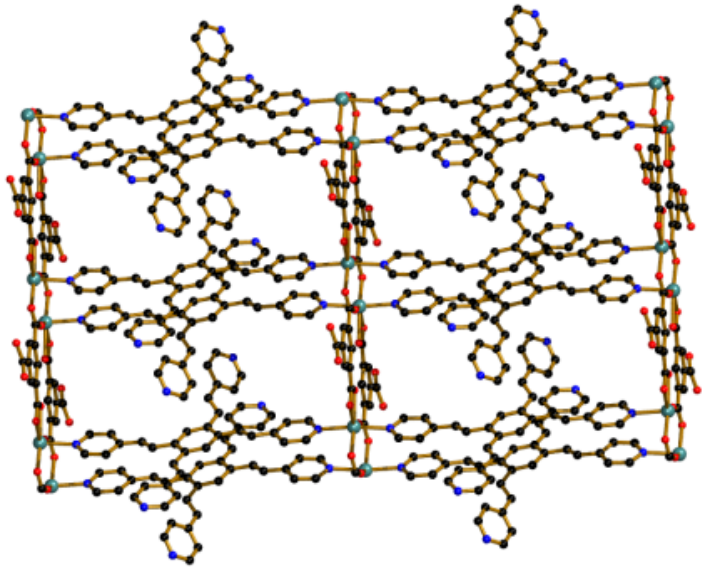

(c)

Fig. S2 (a) View of the coordination environment of the Cd(II) center in **2** with 45% thermal ellipsoids and all hydrogen atoms are omitted for clarity. Symmetry codes: (A) *x*, *y* - 1, *z* + 1; (B) – *x* + 1, - *y*, - *z* + 1; and (C) - *x*+ 2, - *y*, - *z* + 1. (b) View of a section of the 1D double chain $[Cd_2(1,3,5\text{-HBTC})_2]_n$ extending along the *a* axis. (c) View of a 2D network of **2** extending along [0,1,1] plane.

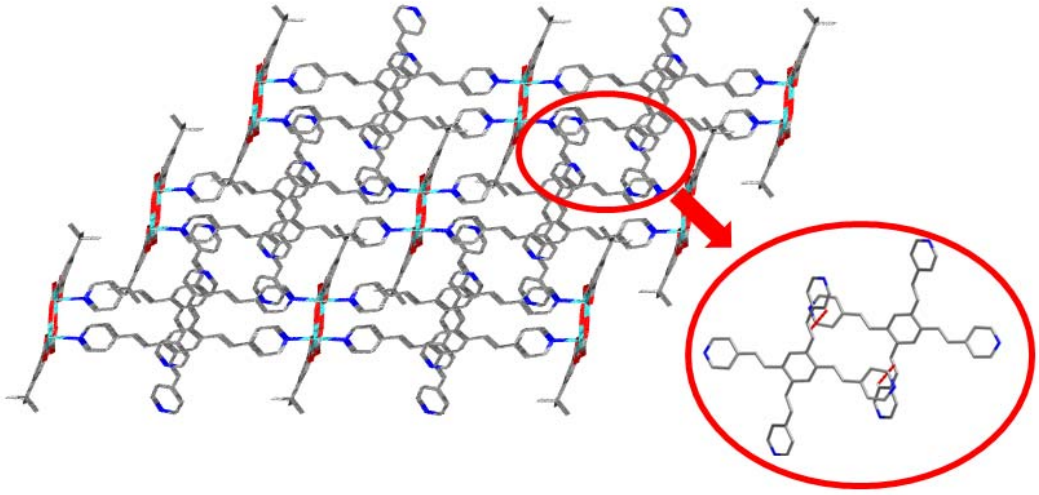

Fig. S3 View of the 3D structure assembled by the π-π stacking interactions in **1**.

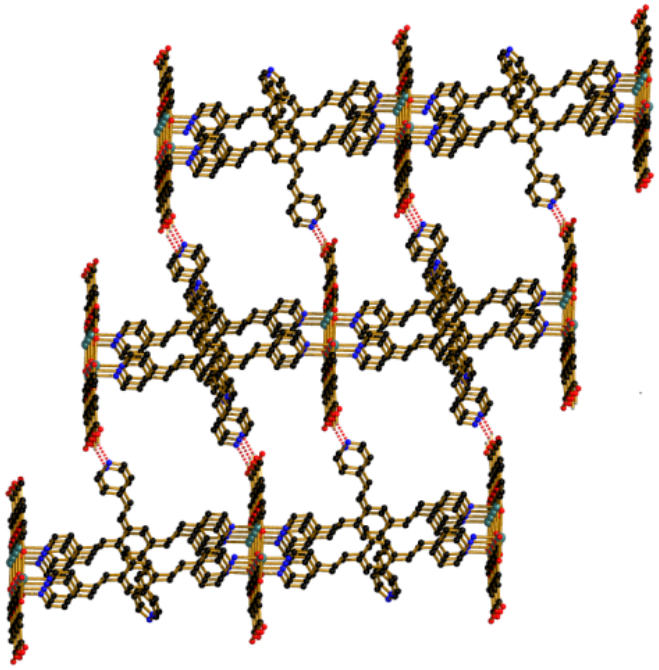

Fig. S4 View of O–H···N hydrogen bonds between two layers of **2**.

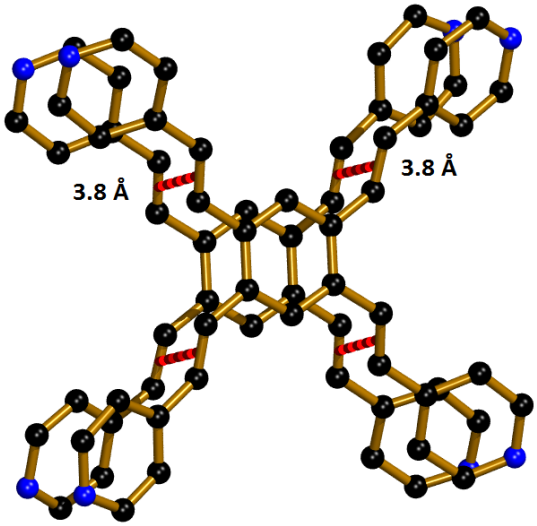

Fig. S5 Alignment of the neighboring 4-tkpvb ligands in **1**.

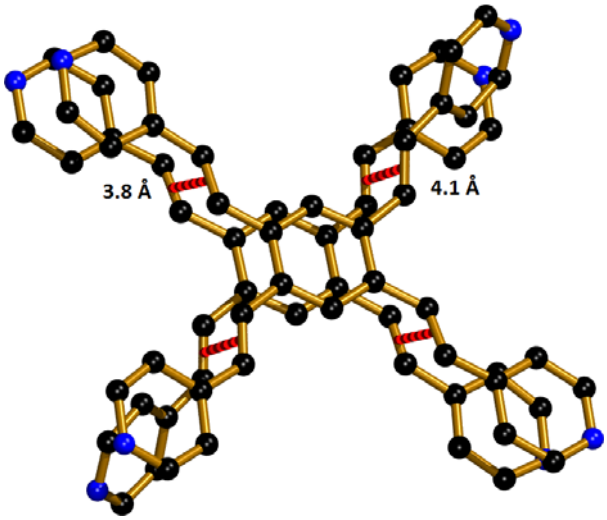

Fig. S6 Alignment of the neighboring 4-tkpvb ligands in **2**.

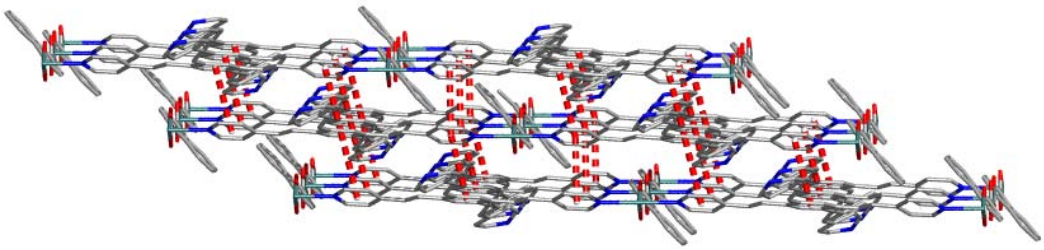

Fig. S7 View of the 3D structure assembled by the π-π stacking interactions in **3**.

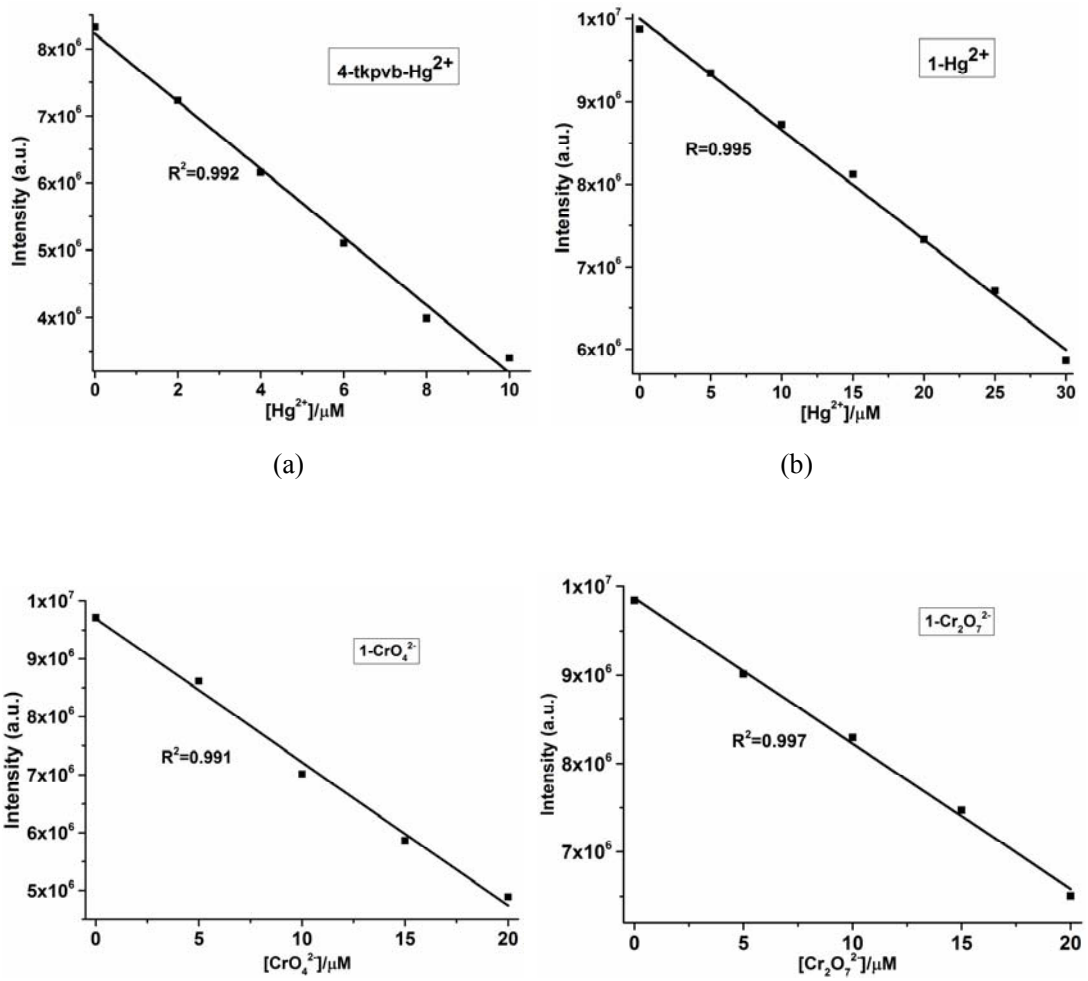

Fig. S8 Linear region of fluorescence intensity for the 4-tkpvb solution and the suspensions of **1** in water upon incremental addition of Hg^{2+}, CrO_4^{2-} or $Cr_2O_7^{2-}$ solutions: (a) 4-tkpvb-Hg^{2+}; (b) **1**-Hg^{2+}; (c) **1**-CrO_4^{2-}; (d) **1**-$Cr_2O_7^{2-}$.

Table S2 Calculation of Detection Limit (LOD)

	4-tkpvb	**1**		
	Hg^{2+}	Hg^{2+}	CrO_4^{2-}	$Cr_2O_7^{2-}$
Standard deviation(δ)	6720	6657	6657	6657
Slope (m, μM^{-1})	5.05×10^5	1.33×10^5	2.48×10^5	1.64×10^5
LOD ($3\delta/m$, μM)	0.04	0.15	0.08	0.12

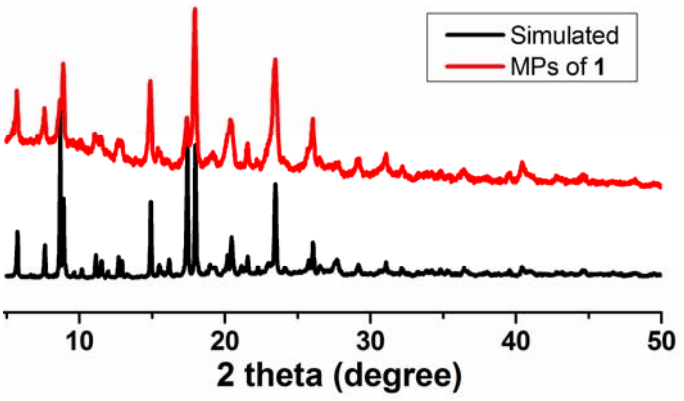

Fig. S9 PXRD patterns of MPs of **1**.

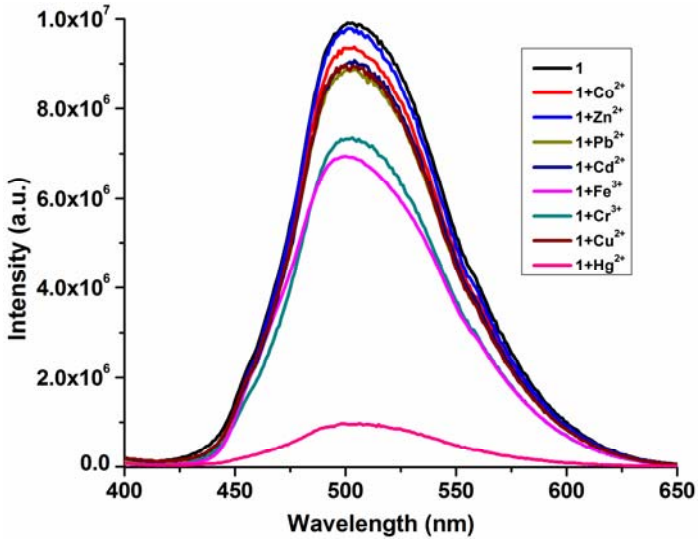

(a)

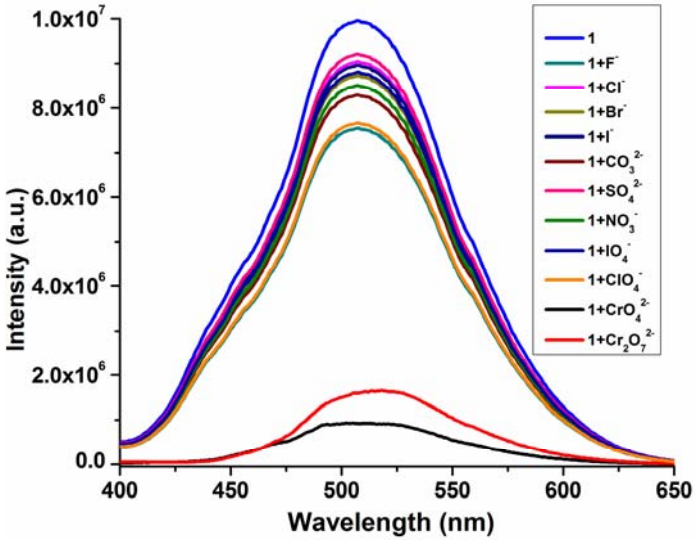

(b)

Fig. S10 Emission spectra of **1** dispersed in water upon addition of inorganic metal ions (a) and anions (b).

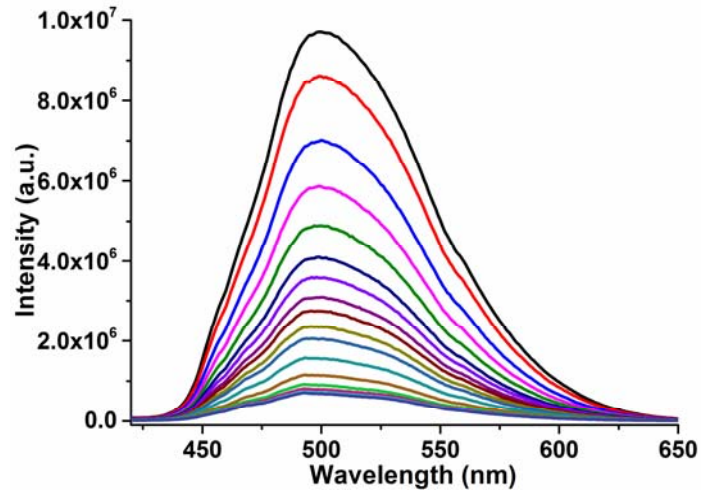

(a)

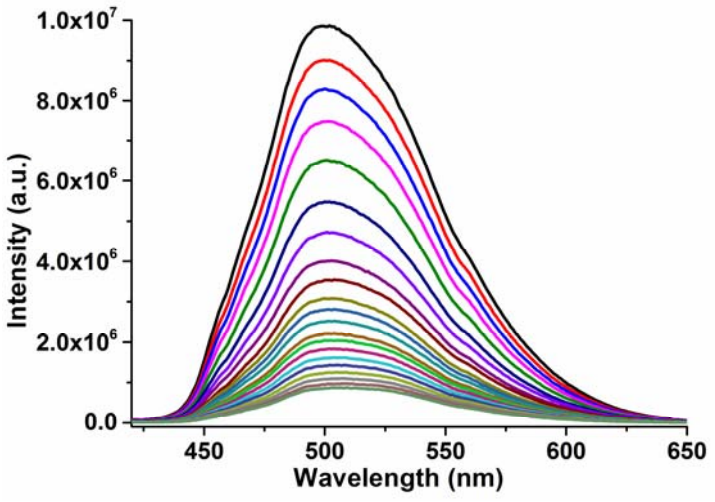

(b)

Fig. S11 Concentration-dependent luminescence quenching of **1** after adding different concentrations of CrO_4^{2-} (a) and $Cr_2O_7^{2-}$ (b).

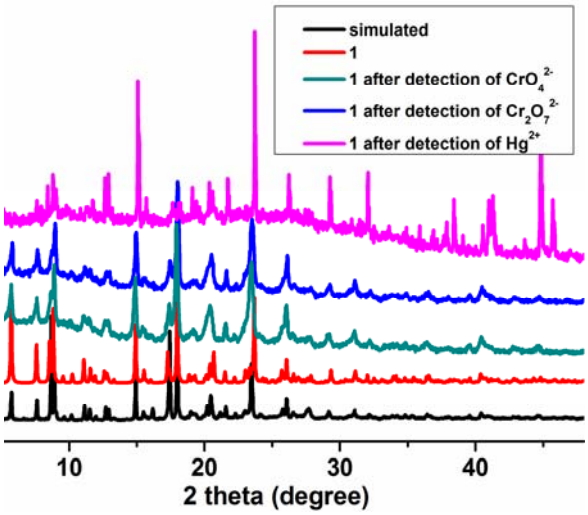

Fig. S12 PXRD patterns for **1** after the detection of Hg^{2+}, CrO_4^{2-} and $Cr_2O_7^{2-}$ in water.

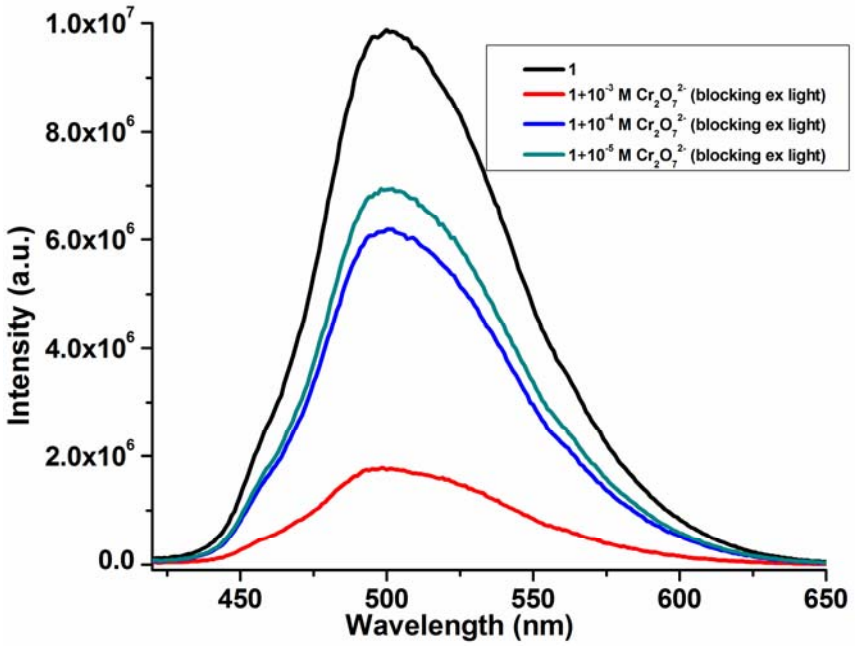

(a)

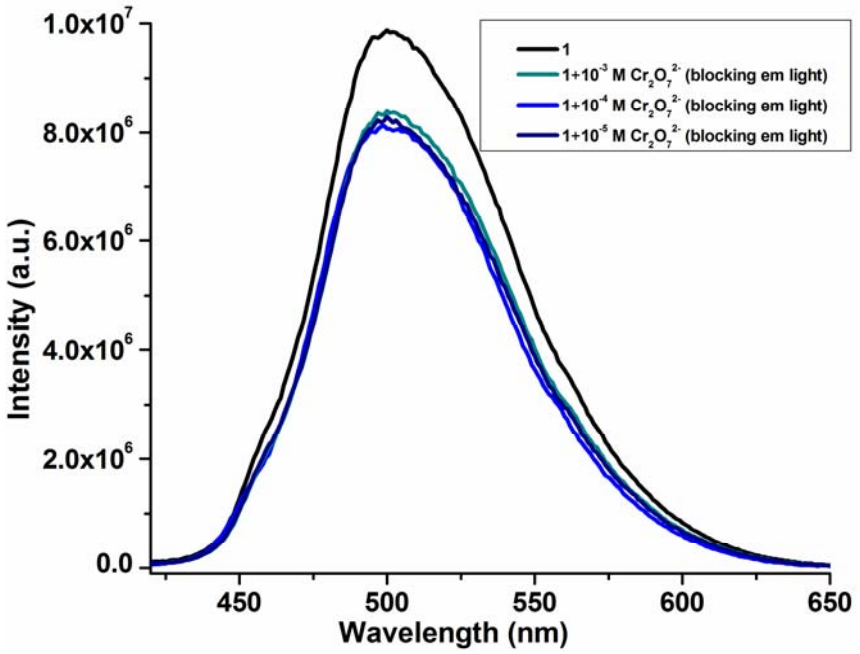

(b)

Fig. S13 Emission spectra of **1** with different concentrations of $Cr_2O_7^{2-}$ covering the excitation light (a) and emission light (b).